Available online at www.sciencedirect.com
ScienceDirect
Thin-Walled Structures 44 (2006) 1175–1184
THIN-WALLED STRUCTURES
www.elsevier.com/locate/tws

Bifurcation of locally buckled point symmetric columns—Experimental investigations

Kim J.R. Rasmussen*

Department of Civil Engineering, School of Civil Engineering, University of Sydney, Sydney, NSW 2006, Australia

Received 6 April 2006; received in revised form 12 September 2006; accepted 12 October 2006
Available online 11 December 2006

Abstract

The bifurcation equations for locally buckled point symmetric sections are derived in a companion paper [Rasmussen KJR. Bifurcation of locally buckled point symmetric columns—analytical developments. Thin-walled Struct, submitted for publication]. In the present paper, two series of experiments are reported, one on narrow flange *Z*-sections and one on wide flange *Z*-sections. The main objective of the tests was to validate the bifurcation load predictions derived in [Rasmussen KJR. Bifurcation of locally buckled point symmetric columns—analytical developments. Thin-walled Struct, submitted for publication] against experimental values. A further objective of the tests on narrow flange sections was to investigate the change in the direction of overall buckling, as predicted by the theory, from principal axis directions to non-principal directions. A further objective of the tests on wide flange sections was to investigate the possible change of the critical overall buckling mode from a flexural mode to a torsional mode as a result of local buckling. Agreement is generally found between analytical and experimental results.

Keywords: *Z*-sections; Steel structures; Tests; Local buckling; Torsional buckling; Flexural buckling; Interaction buckling; Bifurcation analysis; Finite strip analysis; Finite element analysis

1. Introduction

It is well known that local buckling may influence the overall buckling behaviour of thin-walled sections. The influence depends on the end support conditions (e.g. simply supported or fixed) and the symmetry characteristics [1]. For a doubly symmetric section, such as an *I*-section, local buckling reduces the flexural rigidity and precipitates overall buckling at a reduced load but does not induce overall displacements. For a singly symmetric cross-section, such as a channel section, local buckling induces overall bending when the column is compressed between pinned ends but not when compressed between fixed ends [2].

The present paper focuses on the bifurcation of locally buckled point symmetric columns, such as *Z*-section columns, as shown in Fig. 1. Theoretical results [1] have shown that local buckling of point symmetric columns does not induce overall displacements, as it does in pin-ended singly symmetric columns, but causes a coupling between the minor and major axis buckling displacements. In physical terms, this implies that the direction of overall buckling occurs about an axis rotated from the minor principal axis.

According to the theory [1], torsional and flexural overall buckling of point symmetric sections are uncoupled. However, the torsional buckling mode may become critical in the case of *Z*-sections with very slender flanges because local buckling reduces the warping rigidity (EI_ω) more severely than the minor axis flexural rigidity (EI_y). The purpose of this paper is to present tests and finite element analyses of fixed-ended *Z*-section columns to verify experimentally and numerically the behaviour predicted by the theory.

Two test series are reported, one on narrow flange *Z*-sections and one on wide flange *Z*-sections. The tests specimens were manufactured from high strength steel by brake pressing, and so contained low levels of residual stress. Fixed-ended column tests were performed at eight

*Tel.: +61 2 9351 2125; fax: +61 2 9351 3343.
E-mail address: k.rasmussen@civil.usyd.edu.au.

0263-8231/$ - see front matter
doi:10.1016/j.tws.2006.10.009

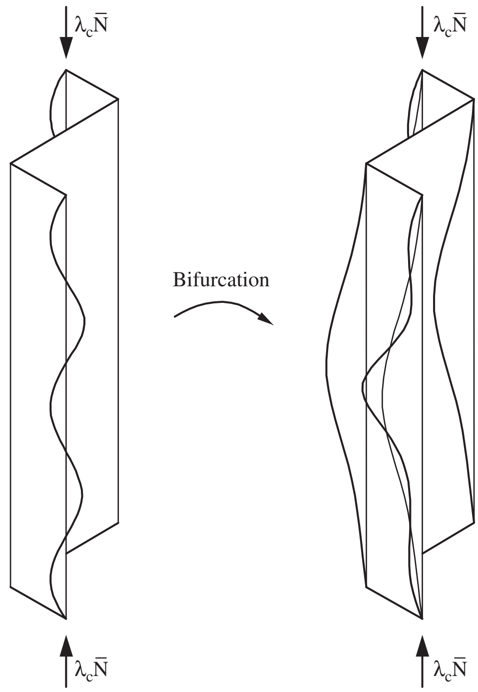

Fig. 1. Overall flexural buckling of locally buckled Z-section. (a) Initial curve and (b) complete curve.

and nine different lengths for the narrow and wide flange test series, respectively, covering the range from stub columns to long columns.

2. Buckling equations

It is shown in a companion paper [1] that the longitudinal buckling displacement w_b, the flexural buckling displacements u_b and v_b in the principal x- and y-axis directions, respectively, and the buckling twist rotation ϕ_b are determined from the differential equations:

$$((EA)_t w_b')' - ((ES_\omega)_t \phi_b'')' = 0, \tag{1}$$

$$-((ES_\omega)_t w_b')'' + ((EI_\omega)_t \phi_b'')'' - ((GJ)_t \phi_b')'' + \left(N_{\rm cr}\frac{\bar{W}}{\bar{N}}\phi_b'\right)' = 0, \tag{2}$$

$$((EI_y)_t u_b'')'' + ((EI_{xy})_t v_b'')'' + (N_{cr} u_b')' = 0, \tag{3}$$

$$((EI_{xy})_t u_b'')'' + ((EI_x)_t v_b'')'' + (N_{cr} v_b') = 0, \tag{4}$$

where N_{cr} is the overall buckling load, $(EA)_t$, $(ES_\omega)_t$, $(EI_x)_t$, $(EI_y)_t$, $(EI_{xy})_t$, $(EI_\omega)_t$, $(GJ)_t$ are tangent rigidities calculated at the buckling load, and

$$\frac{\bar{W}}{\bar{N}} = \frac{\int_A \sigma_0 (x^2 + y^2)\,{\rm d}A}{\int_A \sigma_0\,{\rm d}A}. \tag{5}$$

In Eq. (5), σ_0 is the longitudinal stress at incipient overall buckling. The tangent rigidities ($(EA)_t$, $(ES_\omega)_t$, $(EI_x)_t$, $(EI_y)_t$, $(EI_{xy})_t$, $(EI_\omega)_t$) can be found by subjecting a length of section equal to the local buckle half-wavelength to increasing levels of compression and then superimposing small increments of generalised strain (axial compression, curvature about the major and minor principal axes, and warping) at each compression level. The tangent rigidities are the ratios of the resulting stress resultant to the applied generalised strain, see Refs. [1–3] for details. A nonlinear inelastic finite strip local buckling analysis [4] has been used in this paper to calculate the tangent rigidities.

For fixed-ended columns, the governing Eqs. (1)–(4) and the boundary conditions are satisfied by the displacement field:

$$\frac{w_b}{C_w} = \sin\left(\frac{2\pi z}{L}\right), \tag{6}$$

$$\frac{u_b}{C_u} = \frac{v_b}{C_v} = \frac{\phi_b}{C_\theta} = 1 - \cos\left(\frac{2\pi z}{L}\right), \tag{7}$$

which, upon substitution into Eqs. (1)–(4), leads to an eigenvalue problem with the following non-trivial solutions [1],

$$N_{cr\,\varphi} = \frac{\bar{N}}{\bar{W}}\left(\frac{4\pi^2 (EI_\omega)_t}{L^2} + (GJ)_t - \frac{4\pi^2}{L^2}\frac{(ES_\omega)_t^2}{(EA)_t}\right), \tag{8}$$

$$N_{cr\,uv} = \frac{-B \pm \sqrt{B^2 - 4AC}}{2A}, \tag{9}$$

where

$$A = 1, \tag{10}$$

$$B = -(N_x + N_y), \tag{11}$$

$$C = N_x N_y - \left(\frac{2\pi}{L}\right)^4 (EI_{xy})_t^2, \tag{12}$$

$$N_x = \frac{4\pi^2 (EI_x)_t}{L^2}, \tag{13}$$

$$N_y = \frac{4\pi^2 (EI_y)_t}{L^2}. \tag{14}$$

3. Experimental investigations

3.1. Narrow flange Z-sections

3.1.1. Material properties

The test specimens were brake-pressed into section from nominally 1.5 mm thick G500 sheet steel. G500 is an Australian-produced steel to AS1397 [5] with galvanised coating and nominal yield stress of 500 MPa. It has a low tensile strength to yield stress ratio and limited ductility of the order of 10–15%.

Five tensile coupons were cut from steel sheets in the same direction as the longitudinal axis of the test specimens. Figs. 2a and b show a typical stress–strain curve obtained from one of the coupon tests. The average values of initial Young's modulus (E_0), yield stress (σ_y) and